Title:

Distinct Functions of the Atypical Terminal Hydrophilic Domain of the HKT Transporter in the Liverwort *Marchantia polymorpha*

Running head: Regulation of MpHKT1-mediated ion transport

Corresponding author: T. Horie; Division of Applied Biology, Faculty of Textile Science and Technology, Shinshu University, 3-15-1, Tokida, Ueda, Nagano 386-8567, Japan.

Tel: +81-268-21-5561

Fax: +81-268-21-5556

email: horie@shinshu-u.ac.jp

Subject areas: Membrane and transport

Number of figures and tables: black and white figures (0); color figures (9); tables and type (0); and supplementary material (3, a Power Point file including four figures and two Excel files including a single table)

Title:

Distinct Functions of the Atypical Terminal Hydrophilic Domain of the HKT Transporter in the Liverwort *Marchantia polymorpha*

Running head: Regulation of MpHKT1-mediated ion transport

Shahin Imran[1,2,†], Masumi Oyama[3†], Rie Horie[3], Natsuko I. Kobayashi[4], Alex Costa[5,6], Ryosuke Kumano[3], Chiho Hirata[7], Sen Thi Huong Tran[1,8], Maki Katsuhara[1], Keitaro Tanoi[4], Takayuki Kohchi[9], Kimitsune Ishizaki[7], Tomoaki Horie[3,*]

[1]Institute of Plant Science and Resources, Okayama University, 2-20-1 Chuo, Kurashiki 710-0046, Japan

[2]Department of Agronomy, Khulna Agricultural University, Khulna-9100, Bangladesh

[3]Division of Applied Biology, Faculty of Textile Science and Technology, Shinshu University, 3-15-1 Tokida, Ueda, Nagano 386-8567, Japan

[4]Graduate School of Agricultural and Life Sciences, The University of Tokyo, 1-1-1, Yayoi, Bunkyo-ku, Tokyo 113-8657, Japan

[5]Department of Biosciences, University of Milan, via Celoria 26, 20133 Milano, Italy

[6]Institute of Biophysics, National Research Council of Italy (CNR), 20133 Milano, Italy

[7]Graduate School of Science, Kobe University, Kobe 657-8501, Japan

[8]Faculty of Agronomy, University of Agriculture and Forestry, Hue University, Hue 530000, Vietnam

[9]Graduate School of Biostudies, Kyoto University, Kyoto 606-8502, Japan

*Corresponding author: horie@shinshu-u.ac.jp, +81-268-21-5556 (Fax)

†These authors contributed equally to this work.

Abstract

K^+/Na^+ homeostasis is important for land plants, particularly under salt stress. In this study, the structure and ion transport properties of the high-affinity K^+ uptake transporter (HKT) of the liverwort *Marchantia polymorpha* were investigated. Only one *HKT* gene, Mp*HKT1*, was identified in the genome of *M. polymorpha*. Phylogenetic analysis of HKT proteins revealed that non-seed plants possess HKTs grouped into a clade independent of the other two clades including HKTs of angiosperms. A distinct long hydrophilic domain was found in the C-terminus of MpHKT1. cDNA of truncated Mp*HKT1* (*t*-Mp*HKT1*) encoding the MpHKT_Δ596-812 protein was used to examine the functions of the C-terminal domain. Both MpHKT1 transporters fused with EGFP at the N-terminus were localized to the plasma membrane when expressed in rice protoplasts. Two-electrode voltage clamp experiments using *Xenopus laevis* oocytes indicated that MpHKT1 mediated the transport of monovalent alkali cations with higher selectivity for Na^+ and K^+, but truncation of the C-terminal domain significantly reduced the transport activity with a decrease in the Na^+ permeability. Overexpression of MpHKT1 or t-MpHKT1 in *M. polymorpha* conferred accumulation of higher Na^+ levels and showed higher Na^+ uptake rates, compared to those of wild-type plants, however, phenotypes with t-MpHKT1 were consistently weaker than those with MpHKT1. Together, these findings suggest that the hydrophilic C-terminal domain plays a unique role in the regulation of transport activity and ion selectivity of MpHKT1.

Keywords: HKT, Na^+ transport, K^+ transport, *Marchantia polymorpha*

Introduction

The high-affinity K^+ transporter (HKT) proteins constitute an important transmembrane protein family in plants, and these proteins mediate Na^+ transport across membranes with strong Na^+ selectivity (Horie et al. 2009). HKT proteins have been classified into subfamilies 1 and 2, and the proteins belonging to each subfamily are termed HKT1s and HKT2s, respectively (Horie et al. 2009; Platten et al. 2006). HKT1s mediate Na^+ uniport like a Na^+ selective channel (Xue et al. 2011), several of which contribute to salt tolerance in plants, including Arabidopsis, rice, and maize, by mediating Na^+ exclusion from leaves (Berthomieu et al. 2003; Campbell et al. 2017; Davenport et al. 2007; Kobayashi et al. 2017; Mäser et al. 2002a; Ren et al. 2005; Sunarpi et al. 2005; Wang et al. 2015; Zhang et al. 2018). By contrast, HKT2s show strong selectivity for K^+ as well as for Na^+ (Horie et al. 2009 and references therein). Unlike the robust K^+ transport activity of HKT2s in heterologous expression systems, detection of the HKT2-mediated K^+ transport activity *in planta* is difficult, and the biological significance of K^+-transporting HKT2s remains to be elucidated. The Na^+ transport function of OsHKT2;1 in rice has been genetically demonstrated to contribute to nutritional Na^+ absorption in roots to partially compensate for K^+ deficiency (Horie et al. 2007). A unique physiological role with genetic evidence for the function of K^+ transport through an HKT2 transporter has been proposed in a study on maize and teosinte (Cao et al. 2019). The reduced K^+ transport activity of ZmHKT2 in the plasma membrane (PM) of xylem parenchyma cells was suggested to account for higher K^+ loading in xylem vessels, which consequently increases K^+ accumulation in leaves and thus enhances salt tolerance of the plant (Cao et al. 2019). The functions of the HKT transporter in the moss *Physcomitrium* (*Physcomitrella*) *patens*, i.e., PpHKT1, have been previously reported (Haro et al. 2010). However, the physiological roles of HKT transporters in non-vascular plants are largely unknown, and further knowledge regarding the structure and ion transport properties of such HKT transporters is required.

Liverworts such as *Marchantia polymorpha* are categorized as bryophytes, together with mosses and hornworts. Bryophytes show several distinct characteristics, including the lack of a vascular system and dominance of the photoautotrophic gametophyte generation which is haploid during its life cycle (Ishizaki 2017; Kohchi et al. 2021). *M. polymorpha* has historically been a model plant species in the fields of development, physiology, and genetics (Bowman 2016a). In addition to low genetic redundancy in the *M. polymorpha* genome in comparison with genomes of other land plants (Bowman et al. 2017), recent developments in

anatomy, taxonomy, and molecular genetics have further increased attention to *M. polymorpha* plants as potent models for studying fundamental mechanisms of land plants (Bowman et al. 2016b; Ishizaki et al. 2008; Ishizaki et al. 2015; Ishizaki et al. 2016; Kohchi et al. 2021; Kubota et al. 2013; Saint-Marcoux et al. 2015; Shimamura 2016; Tsuboyama-Tanaka and Kodama 2015).

In this study, we focused on the *HKT* gene in *M. polymorpha* to elucidate the structure and ion transport functions of the product, which may provide important information as a distinct HKT protein of non-vascular plants. We have identified a unique *HKT* homolog in the genome of *M. polymorpha*, i.e., the Mp*HKT1* gene, the encoded protein of which was found to be grouped in a clade independent from those containing HKT1 and HKT2 transporters of angiosperms. The predicted secondary structure of MpHKT1 was characteristic such that a long hydrophilic domain facing the cytosol followed the transmembrane domains, which is not common among HKTs. The effects of the C-terminal domain of MpHKT1 on membrane targeting, ion selectivity, and ion transport activity are discussed.

Results

Identification of the *HKT* gene in the *M. polymorpha* genome and cDNA isolation

The *HKT* gene was searched in the *M. polymorpha* genome database (https://marchantia.info/) using the amino acid sequence of OsHKT2;1 of rice (Horie et al. 2001). One potential locus that encoded a protein showing marked similarity with OsHKT2;1 was highlighted as a result (Mp7g13910). The cDNA was isolated from a male wild-type (WT) of *M. polymorpha*, Takaragaike (Tak)-1, using gene-specific primers (Table S1) and was found to encode 812 amino acids. The deduced amino acid sequence showed approximately 35% identity to that of PpHKT1 of the moss *Physcomitrium patens* (Haro et al. 2010), indicating that the isolated cDNA encoded the HKT protein of *M. polymorpha*. Phylogenetic analysis of HKTs derived from herbaceous plants and bryophytes resulted in the classification of HKTs into three clades, among which the *M. polymorpha* HKT was found to be placed a clade independent of the others (Fig. 1). The identified gene was termed Mp*HKT1* (see Discussion). The prediction of the secondary structure of MpHKT1 resulted in showing 11 transmembrane domains with a characteristic long hydrophilic domain at the C-terminus of MpHKT1, residing in the cytosol (Fig. 2A). An

amino acid sequence alignment of MpHKT1 and PpHKT1 revealed the absence of such a long hydrophilic domain in PpHKT1 (Fig. S1). As a long C-terminal domain is unusual in HKTs, we examined the role of the domain in the mechanism of ion transport. We thus produced an MpHKT1 mutant, in which the C-terminal domain was truncated at the 595th amino acid of MpHKT1 in accordance with the similarity with PpHKT1 (Figs. 2B, S1). The resultant mutant of MpHKT1 is here referred to as truncated-MpHKT1 (t-MpHKT1) (Fig. 2B). Amino acid sequence alignments of some HKTs, including MpHKT1, indicated that the MpHKT1 protein retains four p-loops as other HKTs and the key amino acid residue, glycine (G), relevant to the K^+ and Na^+ selectivity, was maintained in each loop domain (Fig. 2C) (Hauser and Horie 2010; Mäser et al. 2002b).

Subcellular localization of EGFP-fused MpHKT1 transporters in plant cells

DNA constructs for a transient expression assay in plant cells were prepared by cloning Mp*HKT1* and *t*-Mp*HKT1* cDNAs in the transient expression vector, by which EGFP was fused with each MpHKT1 at the N-terminus. DNA constructs to express either EGFP, EGFP-MpHKT1, or EGFP-t-MpHKT1 were introduced into rice protoplasts prepared from shoots of young rice seedlings (Kobayashi et al. 2017; Suzuki et al. 2016). Each construct was co-introduced with a plasmid harboring an expression cassette of CBL1n-OFP, which is a known PM marker (Batistic et al. 2010; Kobayashi et al. 2017; Suzuki et al. 2016). When cells expressing EGFP-MpHKT1 were analyzed using confocal microscopy, EGFP fluorescence was observed in the periphery of the cells, which matched well the fluorescence of CBL1n-OFP (Fig. 3A, D, G, and J). A similar trend was observed regarding cells expressing EGFP-t-MpHKT1; that is, EGFP fluorescence occurred in the cell periphery (Fig. 3A, B white arrows), and it overlapped with OFP fluorescence of the PM marker (Fig. 3B, E, H, and K). In contrast, cells expressing EGFP showed strong fluorescence in the cytosol, which did not overlap with OFP fluorescence (Fig. 3C, F, I, and L). The plot-profile pixel intensity analysis further indicated that EGFP and OFP fluorescence observed in MpHKT1- and t-MpHKT1-expressing cells well overlap in comparison with the case of the cells expressing EGFP alone (Fig. 3J-L). Note that GFP fluorescence also occurred within the cell, in addition to the periphery, in the case of EGFP-MpHKT1- and EGFP-t-MpHKT1-expressing cells (Fig. 3A, B, G, and H). We deduce that some MpHKT1 proteins remained in the endoplasmic reticulum (ER). A similar phenomenon was observed when rice OsHKT1;4 and OsHKT1;5 were expressed in rice protoplasts (Kobayashi et al. 2017;

Suzuki et al. 2016). Taken together, these results indicate that both EGFP-MpHKT1 and EGFP-t-MpHKT1 are localized in the PM of rice protoplasts, thus suggesting PM-localization of MpHKT1 in *M. polymorpha*.

Properties of ion transport mediated by MpHKT1 and t-MpHKT1, expressed in *Xenopus laevis* oocytes

To investigate the characteristics of ion transport through MpHKT1 proteins, cDNAs were subcloned into the pXβG-ev1 vector to produce the corresponding cRNAs. For the two-electrode voltage clamp (TEVC) analysis, *X. laevis* oocytes were injected with either water, 12.5 ng Mp*HKT1* cRNA, or 12.5 ng *t*-Mp*HKT1* cRNA. Current-voltage relationships were obtained in the presence of 96 mM Na^+, K^+, Rb^+, Cs^+, or Li^+ (as chloride salts) and were compared among oocytes injected with Mp*HKT1* cRNA, *t*-Mp*HKT1* cRNA, or water (Fig. 4). Large currents were elicited when MpHKT1-expressing oocytes were bathed in the solutions in comparison with water-injected oocytes although the current amplitudes were variable depending on the cation (Fig. 4A, B). These results indicated that MpHKT1 shows broad selectivity for monovalent alkali cations. The reversal potentials obtained in the experiment, listed in Table S2, suggested selectivity of MpHKT1 for the cations in the order $Na^+ > K^+ > Rb^+ > Cs^+ > Li^+$ (Fig. 4B). The data also indicated that current amplitudes observed in MpHKT1-expressing oocytes were particularly higher in Na^+, K^+ and Rb^+ baths (Fig. 4A, B). By contrast, truncation of a part of the C-terminus led to different outcomes: t-MpHKT1 expression in oocytes elicited currents in all tested bath solutions as MpHKT1; however, the magnitude of the currents was largely reduced, and the selectivity of t-MpHKT1 for monovalent alkali cations was not completely identical to that of MpHKT1 (Fig. 4, Table S2). To further investigate the selectivity of MpHKT1 for Na^+, the concentration of Na^+ in the external solution was changed from 96 to 9.6 mM. The reversal potentials of MpHKT1-expressing oocytes bathed in a 96 mM NaCl and a 9.6 mM NaCl (supplemented with 86.4 mM choline chloride) solution were of, respectively, -3.0 ± 0.7 mV and -50.6 ± 2.3 mV (n=10-12, ± SE) (Fig. S2A). Moreover, no notable difference was observed in MpHKT1-mediated currents between 96 mM NaCl and a solution containing 9.6 mM NaCl and 86.4 mM Na-glutamate (Fig. S2A). That is, an approximately 47-mV shift in the reversal potential was observed upon a ten-fold increase in the Na^+ concentration, which was slightly less than a Nernstian shift (approximately 58 mV at 20°C). These results indicated that MpHKT1 mediated Na^+ transport, and the influence of Cl^- was negligible. Based on the comparison with the water-injected control, t-MpHKT1-expressing oocytes elicited

currents with all tested monovalent cation salts (Fig. S2B, C). However, in contrast to oocytes expressing MpHKT1, a decrease in the extracellular Na^+ concentration did not trigger a significant shift in the reversal potential (Fig. S2B), implying that Na^+ selectivity of t-MpHKT1 differed from that of the full-length protein.

Currents mediated by MpHKT1 and t-MpHKT1 were then recorded using solutions with combinations of different monovalent cations. Current-voltage relationships obtained from MpHKT1 expressed in oocytes indicated that addition of 24 mM K^+, but not of 24 mM Rb^+, Cs^+, and Li^+, significantly increased the currents and ionic conductance of MpHKT1 as in the case of an increase of 24 mM Na^+ in the presence of 72 mM Na^+ (Fig. 5A, C). These observations suggest higher selectivity for Na^+ and K^+ by MpHKT1. In contrast, t-MpHKT1 showed no difference in their ionic currents and conductance when a 24 mM monovalent alkali cation salt was added to the bath solution including 72 mM NaCl (Fig. 5B, D). When similar experiments were performed using a bath solution containing 72 mM KCl, addition of a 24 mM monovalent alkali cation salt did not induce a significant difference in MpHKT1-mediated currents and ionic conductance (Fig. S3A, S3C). Similar results were obtained when t-MpHKT1-expressing oocytes were used for TEVC recordings under the same solution conditions (Fig. S3B, S3D).

Mp*HKT1* expression in *M. polymorpha*

Mp*HKT1* mRNA abundance was investigated by quantitative PCR (qPCR) using gene-specific primers (Table S1). Male and female WT accessions of *M. polymorpha* (Tak-1 and Tak-2, respectively) were grown on K^+-rich (15 mM) or K^+-deficient (0.05 mM) medium with or without 50 mM NaCl. Total RNA was extracted from each accession for qPCR analysis. Overall, Mp*HKT1* mRNA accumulation under K^+-rich conditions was significantly higher than that under K^+-deficient conditions (Fig. 6A). A one-week salt stress treatment tended to slightly increase the level of Mp*HKT1* mRNA in the presence of 15 mM K^+, and there was no notable difference in Mp*HKT1* mRNA levels between Tak-1 and Tak-2 under K^+-rich conditions (Fig. 6A). Under K^+-deficient conditions, the amount of Mp*HKT1* mRNA was approximately 10–42% of that under K^+-rich conditions (Fig. 6A). The only difference in Mp*HKT1* mRNA levels between Tak-1 and Tak-2 under K^+-deficient conditions was observed after salt stress, as Mp*HKT1* mRNA abundance in Tak-1 was significantly higher than that in Tak-2 (Fig. 6A).

Characterization of transgenic *M. polymorpha* plants overexpressing Mp*HKT1* cDNAs

To understand the function of MpHKT1 *in vivo*, *M. polymorpha* plants over-expressing MpHKT1 or t-MpHKT1 were used. Two independent transgenic lines were produced for each construct, and the expression levels of the transgene were analyzed by qPCR. The lines overexpressing Mp*HKT1* (OE1, 2) and *t*-Mp*HKT1* (t-OE1, 2) showed approximately 5- to 12-fold and 33- to 34-fold increases in mRNA levels, respectively, compared with the WT line Tak-1 (Fig. 6B).

Na^+ and K^+ contents of these transgenic lines were measured under K^+-rich (15 mM) and low K^+ (0.5 mM) conditions with or without 50 mM NaCl. At 15 mM K^+, no difference was found in the K^+ content among WT, OE, and t-OE lines (Fig. 7C). However, regarding Na^+ content, OE and t-OE lines accumulated significantly more Na^+ than WT plants, which was presumably stimulated by a few mM Na^+ added for pH adjustment (Fig. 7A). A one-week salt stress treatment with 50 mM NaCl led to approximately 5- to 8-fold increases in Na^+ content in all lines, however, the accumulation profiles were similar to those of the controls; that is, OE and t-OE lines accumulated significantly more Na^+ than WT, among which OE lines showed the highest Na^+ content (Fig. 7B). The salt stress treatment in general reduced the K^+ content in all lines (Fig. 7C, D). In particular, OE and t-OE lines accumulated significantly less K^+ than WT, and approximately 80% and 56% reductions in the K^+ content of OE and t-OE lines were observed, respectively, compared with those under K^+-rich control conditions (Fig. 7C, D). At 0.5 mM K^+, control and salt stress conditions led to similar profiles of Na^+ and K^+ contents in WT, OE, and t-OE lines as those with 15 mM K^+ (Fig. 7E-H). Incubation with 0.5 mM K^+ resulted in the highest Na^+ accumulation in the two OE lines, showing a significant difference in the K^+ content compared with the other lines (Fig. 7E, G). Under salt stress, both OE and t-OE lines accumulated significantly more Na^+ than WT, and the two OE lines tended to accumulate it at the highest level (Fig. 7F). By contrast, the K^+ content of OE lines upon salt stress was lowest, which was reduced by approximately 80%, compared with the 0.5 mM K^+ treatment (Fig. 7G, H). t-OE lines showed significantly higher K^+ content than OE lines, however, they showed approximately 38–40% reductions in comparison with the controls (Fig. 7G, H).

Growth defects in OE lines became prominent when all *M. polymorpha* lines were subjected to longer periods of salt stress with 50 mM Na^+ (three weeks), particularly in combination with 0.5 mM K^+ (Fig. 8). No notable differences in visual and fresh weights were observed between male WT and transgenic lines (Fig. 8A, C). However, salt stress had a significant negative effect on growth in OE lines, but not on that of WT and t-OE lines (Fig. 8B, D). These results suggest that Na^+ transport mediated by MpHKT1 increased the salt sensitivity of OE lines under the salt stress condition tested.

We also performed $^{22}Na^+$ tracer experiments using the WT and transgenic lines. Six individuals per line were prepared in a K^+-rich medium. All lines were incubated on fresh low-K^+ medium supplemented with 50 mM NaCl and an appropriate amount of $^{22}NaCl$ for 1 h. An image of the labeled plants was obtained after exposure to an imaging plate (IP) (Fig. 9A). Based on the IP image, Na^+ uptake rates of all lines were calculated, and both OE lines showed significantly higher Na^+ uptake rates, compared to WT lines (Fig. 9B). By contrast, t-OE lines showed increasing trends regarding Na^+ uptake rates, compared with that of WT, however, the differences were not statistically significant (Fig. 9B).

Discussion

Identification of the *HKT* gene in *M. polymorpha*

The liverwort *M. polymorpha* belongs to the earliest diverging group of land plants and is becoming an important model plant because of the development of experimental methods and its simple genome structure, which offers opportunities to understand the molecular physiological function of various genes of interest (Bowman et al. 2017; Ishizaki et al. 2015; Kohchi et al. 2021). In this study, the *HKT* gene in *M. polymorpha* was focused because of the significant relevance of HKT proteins in the transport of K^+ and Na^+, the accumulation of which can be important parameters regarding salt sensitivity in plants (Ismail and Horie 2017; Karahara and Horie 2021). Based on the search for the *HKT* gene in the genome database of *M. polymorpha* with reference to the amino acid sequence of OsHKT2;1 in rice, only one gene was considered as an *HKT* ortholog (Mp7g13910). Based on the cDNA, this gene was deduced to encode a membrane protein with the length of 812 amino acids, which is highly identical to PpHKT1 of the moss *P. patens* (Fig. S1). We thus termed

this gene Mp*HKT1*. Phylogenetic analysis of HKTs of land plants revealed that MpHKT1 is grouped in a clade with HKTs from non-seed plants, independent of the clades including HKT1s and HKT2s of angiosperms (Fig. 1). This result suggests that HKTs from non-seed plants may be categorized as an independent subgroup of HKT transporters of land plants (Fig. 1), which may be referred to as subfamily 3. Previous studies proposed similar conclusions (Hauser and Horie 2010; Su et al. 2015). Plant HKT proteins have been suggested to retain a selectivity pore that is distantly homologous to that of a bacterial K^+ channel (KcsA) and to belong to a large cation transporter family which occurs in the kingdoms of fungi, bacteria, and plants, i.e., the Trk/Ktr/HKT family (Corratgé-Faillie et al. 2010; Durell and Guy 1999; Durell et al. 1999; Hauser and Horie 2010). HKTs of non-seed plants might share distinct characteristics regarding cation transport and structure, which could be more similar to procaryotic/fungal Trk/Ktr transporters in comparison with those of HKTs from angiosperms. To discern such possibilities, gaining knowledge of structure, ion selectivity, and phylogenetic relationships of HKTs in various non-seed plants as well as of Trk/Ktr transporters in procaryotes and fungi (Corratgé et al. 2007) is indispensable.

Structural characteristics of MpHKT1 and effects on ion transport

A long hydrophilic domain at the C-terminus is a distinct structural characteristic of MpHKT1 (Fig. 2A), as such a long hydrophilic terminal domain has not been recognized in other HKTs of angiosperms so far. The deduced secondary structure and the amino acid sequence of PpHKT1, which belongs to the same clade as MpHKT1 (Fig. 1), did not show a long hydrophilic C-terminal tail similar to that of MpHKT1 (Fig. S1). Looking into the tail of SmHKT1 proteins in the same clade (Fig. 1), none of them had a long tail as MpHKT1: at most, one of the SmHKT1 proteins EFJ21973.1 showed a longer tail than the others, which was approximately two-fifths of the tail of MpHKT1. To understand the function of the long C-terminal domain of MpHKT1, artificial Mp*HKT1* cDNA (i.e., *t*-Mp*HKT1*) that encodes a protein of 595 amino acids, lacking most of the C-terminal domain (596-812 amino acids), was produced based on an amino acid alignment of MpHKT1 and PpHKT1 (Figs. 2B, S1). Robust ion transport activity of MpHKT1 expressed in *X. laevis* oocytes was detected in the presence of 96 mM monovalent alkali cations with higher selectivity for Na^+ and K^+ (Figs. 4A, 4B, 5A, 5C, S2A, and S2C). Interestingly, the same sets of TEVC experiments using oocytes expressing t-MpHKT1 provided evidence that

truncation of the C-terminal domain of MpHKT1 caused significant reductions in ionic conductance and disturbed ion selectivity (Figs. 4, 5, S2). Overexpression of MpHKT1 and t-MpHKT1 in *M. polymorpha* suggested robust Na^+ transport mediated by MpHKT1 transporters such that OE and t-OE accumulated significantly more Na^+ than male WT (i.e., Tak-1), independent of the amount of external K^+ and the presence of a large amount of Na^+ (Fig. 7A, B, E, and F). Note, however, that Na^+ accumulation was consistently higher in OE lines than in t-OE lines, even though the level of Mp*HKT1* mRNA in t-OE lines was significantly higher than that in OE lines (Fig. 6B). Furthermore, only OE lines but not WT and t-OE lines showed severe salt sensitivity in terms of visual signs and fresh weight in the presence of 0.5 mM K^+ and 50 mM Na^+ (Fig. 8B, D), indicating that Na^+ transport through full-length MpHKT1 triggered Na^+ toxicity in *M. polymorpha* under salt stress. Na^+ concentrations were increased by approximately 146–150% in OE lines, compared with WT, whereas those of t-OE lines were 94–96% under the 0.5 mM K^+ and 50 mM Na^+ condition (Fig. 7F). By contrast, K^+ concentrations were reduced by approximately 75% and 32–35% in OE and t-OE lines, respectively (Fig. 7H). As a result, the K/Na concentration ratios of OE and t-OE lines ended up with approximately 0.06 and 0.35−0.37, respectively. Although the ratios of t-OE lines were lower than those of WT (1.05), the difference in the K/Na ratio between OE and t-OE lines may be one of the major reasons for the phenotypic differences shown in Figure 8. Additional TEVC experiments with similar Na^+ and K^+ concentrations and pH as the characterization of transgenic *M. polymorpha* lines indicated the following: (i) strong selectivity of both MpHKT1 transporters for Na^+ in the presence of 50 mM Na^+; and (ii) a substantial reduction in currents mediated by t-MpHKT1 in comparison with those mediated by MpHKT1 (Fig. S4). These results lead to the conclusion that MpHKT1 mediates higher Na^+ transport activity in *M. polymorpha in vivo* because of the long C-terminal domain; moreover, radioactive tracer experiments using $^{22}NaCl$ revealed that the Na^+ uptake rate of the two OE lines was higher than that of the other lines (Fig. 9B), which also supports this conclusion. It should be noted that the difference in ion transport activity between MpHKT1 and t-MpHKT1 was unlikely due to a defect in membrane-targeting by t-MpHKT1, as no significant difference was found in the PM localization of both MpHKT1 transporters fused with EGFP in rice protoplasts (Fig. 3). Taken together, we conclude that the long hydrophilic region at the C-terminus of MpHKT1 is necessary for maximizing ion transport activity and proper ion selectivity. However, the underlying molecular mechanisms remain to be clarified.

The physiological role of MpHKT1 in *M. polymorpha*

In this study, we examined the characteristics of ion transport through MpHKT1 and provided evidence for the importance of the C-terminal hydrophilic domain in the mechanism of MpHKT1-mediated ion transport. However, we were unable to comprehensively elucidate the physiological role of the Mp*HKT1* gene in *M. polymorpha*. In angiosperms, several HKT1 transporters belonging to subfamily 1 showed Na^+ selective transport (Horie et al. 2009; Ismail and Horie 2017, and references therein). Several HKT1 transporters were found to play an essential role in Na^+ exclusion from leaves, which is an essential salt tolerance mechanism (Karahara and Horie 2021 and references therein). More recently, the *SvHKT1;1* gene in the halophytic turf grass *Sporobolus virginicus* was suggested to contribute to the regulation of shoot Na^+ concentrations under salt stress (Kawakami et al. 2020). HKT2 transporters in general showed strong selectivity for K^+ and Na^+, but some HKT2s such as TaHKT2;1 in wheat (Gassmann et al. 1996) and Po-OsHKT2;2 in a salt tolerant indica rice (Horie et al. 2001) mediated robust transport only for Na^+ in the presence of a 100 mM alkali cation, Na^+, K^+, Rb^+, Li^+, or Cs^+, as AtHKT1;1, a subfamily 1 transporter in Arabidopsis (Uozumi et al. 2000). These characteristics were not found in MpHKT1 as it showed broader selectivity for alkali cations in a similar experimental condition (Fig. 3B). On the one hand, the physiological role of OsHKT2;1, one of subfamily 2 transporters in rice, has been proven with genetic evidence that it mediates Na^+ influx into roots under K^+-limited conditions, by which K^+-starvation is partially compensated by absorbed Na^+ ions (Horie et al. 2007). But on the other hand, the physiological roles of the majority of K^+-transporting HKT2s remain unclear. PpHKT1, which belongs to the same subfamily as MpHKT1 (Fig. 1), mediates Na^+ and K^+ uptake in yeast, however, detailed ion transport properties and the exact physiological role of this transporter in *P. patens* is yet to be determined (Haro et al. 2010).

The key amino acid residue Gly, which has been hypothesized to be originated from the GYG motif of the bacterial K^+ channel, was maintained in the four p-loop domains (Fig. 2C, arrowheads) of MpHKT1, suggesting that MpHKT1 is a K^+-permeable transporter as major HKT2s in angiosperms (Mäser et al. 2002b; Riedelsberger et al. 2021). Indeed, robust K^+ transport activity with K^+ currents as strong as Na^+ currents by MpHKT1 was observed when expressed in *X. laevis* oocytes (Figs. 4, 5). In contrast to Na^+, no signs of K^+ transport (e.g., increased K^+ concentrations) were observed in MpHKT1- or t-MpHKT1-overexpressing *M. polymorpha* (Fig. 7). We predicted MpHKT1-stimulated K^+ accumulation under 15 mM or 0.5 mM K^+

conditions as the medium contained only a small amount of Na^+, however, no significant increase or difference in K^+ accumulation was observed (Fig. 7C, G). In fact, the difficulty of detecting HKT2 transporter-mediated K^+ transport in plants has been suggested by studies using transgenic plants harboring an antisense-*TaHKT2;1* construct (wheat) or an *HvHKT2;1*-overexpression construct (barley) (Laurie et al. 2002; Mian et al. 2011). One successful study used tobacco bright yellow 2 (BY2) cultured cells, and K^+-permeable Po-OsHKT2;2 from a salt-tolerant indica rice landrace was overexpressed in BY2 cells, which led to significant increases in the accumulation and influx of Rb^+, which is an analog of K^+ (Yao et al. 2010). The reason why MpHKT1-mediated K^+ transport in *M. polymorpha* was not observed is not yet clear, however, redundancy of the K^+-transporting system in *M. polymorpha* might mask additional K^+ transport activity, brought about by overexpression of MpHKT1 transporters. Mp*HKT1*-knockout lines using Tak-1 or Tak-2 plants (Kubota et al. 2013) will be required for detailed analysis of the physiological roles of this transporter in *M. polymorpha*. To this end, the analysis of tissue-specific expression of MpHKT1 in *M. polymorpha* will also be indispensable.

Materials and Methods

Plant materials and growth conditions

Male and female accessions (Tak-1 and Tak-2, respectively) of *Marchantia polymorpha* L. were asexually cultured as reported previously (Ishizaki et al. 2008). In brief, both accessions were maintained on a half-strength Gamborg's B5 medium (Gamborg et al. 1968) containing 0.5 g/L MES and 1% (w/v) agar (pH 5.7 adjusted by NaOH) under white fluorescent light with a 14:10 h light/ dark cycle at 22°C. Low-K^+ medium plates were prepared by replacing KNO_3 with an equimolar NH_4NO_3 solution. For stress treatments based on qPCR and inductively coupled plasma (ICP) analyses, sterilized gemmae were spread on a normal medium and were cultured for two weeks. Elite gametophytes were transferred to a nylon mesh opening 10 μm (Spectra/Mesh, Spectrum Labs, USA) and were placed on fresh medium for 10 days. Then, each nylon mesh with gametophytes was transferred to control and stress medium plates which were then incubated for five days (for qPCR), one week (for ICP measurements), or three weeks (for evaluation of salt sensitivity and fresh weights). Agrobacterium-mediated transformation of *M. polymorpha* was performed using regenerating thalli, as reported previously (Kubota et al. 2013). Rice (*Oryza sativa* L. cv. Nipponbare) was used for subcellular

localization analysis of MpHKT1 transporters fused with EGFP. Rice seedlings were prepared as previously described (Kobayashi et al. 2017).

Cloning of Mp*HKT1* cDNAs

Based on the genomic DNA sequence of the candidate region in *M. polymorpha*, primers were designed in the putative UTR regions to isolate cDNA (Table S1). Phusion High-Fidelity DNA Polymerase (Thermo Fisher Scientific, USA) was used under the following conditions: 98°C for 2 min, followed by 35 cycles of 98°C for 10 sec, 65°C for 15 sec, and 72°C for 75 sec, and a final step of 72°C for 5 min. The amplified cDNA was extracted from agarose gel using the FastGene Gel/PCR Extraction Kit (NIPPON Genetics, Japan) and was then phosphorylated by using T4 polynucleotide kinase (Takara, Japan). The fragments were subcloned into the EcoRV site of the pBluescript II SK vector. *t*-Mp*HKT1* cDNA, the encoded protein of which lacks a part of the C-terminal domain (Δ596–812), was produced using specific primers (Table S1). pSK::Mp*HKT1* cDNA was used as a template for the PCR reaction using Phusion High-Fidelity DNA Polymerase with the same reaction steps as above, and the fragments were subcloned into pSK, similar to the Mp*HKT1* cDNA protocol.

To identify the subcellular localization of EGFP-fused MpHKT1, Mp*HKT1* and *t*-Mp*HKT1* cDNAs were amplified using Phusion High-Fidelity DNA Polymerase and the *Xba*I site-attached forward and *Xma*I site-attached reverse primers (Table S1). The amplified fragments were subcloned downstream of EGFP in-frame in the pBI221 vector, which was digested with *Xba*I and *Xma*I (Horie et al. 2007).

For the TEVC assay, Mp*HKT1* and *t*-Mp*HKT1* cDNAs were amplified using Phusion High-Fidelity DNA Polymerase and *Bgl*II site-attached primers (Table S1). The amplified fragments were subcloned into the *Bgl*II site of the pXβG-ev1 vector (Preston et al. 1992).

To achieve overexpression of MpHKT1 and t-MpHKT1 in *M. polymorpha*, Mp*HKT1* cDNAs were subcloned into the pMpGWB108 vector (Ishizaki et al. 2015). Mp*HKT1* and *t*-Mp*HKT1* cDNAs were amplified using Phusion High-Fidelity DNA Polymerase and the *Xmn*I site-attached forward and *Not*I site-attached reverse primers (Table S1). The amplified fragments were subcloned into the pENTR2B vector (Thermo Fisher

Scientific), which was digested with *Xmn*I and *Not*I for the subsequent Gateway cloning of the fragments into pMpGWB108.

RNA extraction, reverse transcription, and qPCR analysis

Total RNA was extracted from *M. polymorpha* lines grown on half-strength Gamborg's B5 medium plates using the RNeasy Plant Mini Kit (Qiagen, Limburg, the Netherlands), and qPCR analysis was performed as described previously (Suzuki et al. 2016) using gene-specific primers for the Mp*HKT1* and Mp*EF1α* genes (Table S1). The PCR reaction was performed as follows: 95°C for 30 sec, followed by 40 cycles of 94°C for 5 sec, 63.5°C for 30 sec, and 72°C for 30 sec and a final step of 72°C for 5 min; thereafter, 95°C for 1 min, 60°C for 30 sec, and 98°C for 15 sec.

Subcellular localization analysis using rice protoplasts

Subcellular localization analysis was performed using protoplasts from rice leaf sheaths as described previously (Kobayashi et al. 2017; Suzuki et al. 2016). Briefly, leaf sheath protoplasts were isolated from seven-day-old rice seedlings. The plasmid solution containing the PM marker CBL1n-OFP (Held et al. 2011) was mixed with a solution containing either pBI221::*EGFP*-Mp*HKT1* cDNA, pBI221::*EGFP-t*-Mp*HKT1* cDNA, or pBI221::*EGFP* and was added to isolated protoplasts, followed by the addition of polyethylene glycol (PEG 4000) solution. The protoplasts were re-suspended in WI solution (0.5 M mannitol, 20 mM KCl, and 4 mM MES; pH 5.7) and were kept in the dark at 24°C (Zhang et al. 2011). Confocal microscopy was performed, and images were obtained using an Olympus FluoView 1000 inverted laser scanning confocal imaging system (Olympus, Japan). The plot-profile pixel intensity analysis was performed as described previously (Suzuki et al., 2016).

TEVC experiments using *X. laevis* oocytes

cRNA was synthesized *in vitro* from linearized pXβG-ev1::Mp*HKT1* cDNA and pXβG-ev1::*t*-Mp*HKT1* cDNA using the mMESSAGE mMACHINE T3 kit (Invitrogen, USA). Oocytes were isolated and were injected with 12.5 ng/50 nL Mp*HKT1* or *t*-Mp*HKT1*cRNA, or with 50 nL nuclease-free water; the oocytes were then incubated at 18 ˚C in modified Barth's solution (88 mM NaCl, 1 mM KCl, 2.4 mM $NaHCO_3$, 15 mM Tris-HCl (pH 7.6), 0.3 mM $Ca(NO_3)_2$, 0.41 mM $CaCl_2$, 0.82 mM $MgSO_4$, 10 μg/mL sodium penicillin, and 10 μg/mL streptomycin sulfate until electrophysiological recordings were initiated. Currents were recorded using the TEVC technique one to two days after injection with cRNAs. TEVC recordings and data analyses were performed using an Axoclamp 900A amplifier, an Axon Instruments Digidata 1440A, Clampex 10.3, and Clampfit 10.3 (Molecular Devices, USA). All bath solutions contained 1.8 mM $MgCl_2$ and 1.8 mM $CaCl_2$. HEPES (10 mM) was used as a buffer for the alkali cation analyses, and the pH was adjusted to 7.5 using Tris (Figs. 4, 5, S2, and S3). MES (10 mM) was added as a buffer for the analyses of the Na^+ selectivity in the presence of either 15 mM or 0.5 mM K^+, and the pH was adjusted to 5.5 using bis-tris propane (Fig. S4). All monovalent cations were added as chloride salts. D-mannitol and choline chloride were added when necessary to adjust the osmolality (200–220 mOsm) and to balance ionic strength. Voltage steps (2 sec) were applied from +30 to −150 mV in 15-mV decrements. All experiments were performed at room temperature (20–22°C). Statistical analyses were performed using IBM SPSS Statistics version 25 (IBM, USA). Significant differences were identified by one-way analysis of variance followed by Tukey's HSD.

Measurement of ion content

Ion concentrations in *M. polymorpha* plants were measured as described by Suzuki et al. (2016). In brief, *M. polymorpha* plants were carefully detached from the nylon mesh and were washed twice using ultrapure water (2 min each time). Then, all samples were dried at 65°C for one day, were digested using ultrapure nitric acid (Kanto Chemical, Japan) for one day, and were then boiled three times at 95°C for 10 min. Ion content was determined using an inductively coupled plasma optical emission spectrometer (ICP-OES; SPS3100, SII Nano Technology, Japan).

Na^+ influx experiments using $^{22}NaCl$

M. polymorpha plants were placed on an uptake medium almost identical to the growth medium but containing 0.5 mM K^+, 50 mM Na^+, $^{22}Na^+$ (1.85 kBq/mL), and 0.35% agar. As the uptake medium was soft, the rhizoid side of the plants was in contact with the medium. Sodium uptake assays were performed in a plant growth chamber at 22°C for 1 h. After this, labeled plants were rinsed in a solution identical to the uptake medium but without $^{22}Na^+$ and agar, were carefully dried using with paper towels, and were weighed. Labeled plants were arranged on a paper sheet and were wrapped in plastic wrap. The samples were then exposed to an imaging plate (BAS-IP MS, GE Healthcare UK, Buckinghamshire, UK) and were scanned using an FLA-5000 imaging system (Fujifilm, Tokyo, Japan). Based on radioactivity, the sodium uptake rate (nmol mg^{-1} h^{-1}) was calculated.

Data Availability

The DNA sequence of the Mp*HKT1* gene was deposited in DNA Data Bank of Japan（DDBJ）and the accession number is as follows: LC654238.

Funding

This work was supported by the Ministry of Education, Culture, Sports, Science and Technology (MEXT) of Japan to T.H. [grant number 25119709], MEXT as part of the Joint Research Program implemented at the Institute of Plant Science and Resources, Okayama University in Japan to T.H. [grant numbers 2622, 3019], and the grant-on-aid by Shinshu University in Japan to T.H. and A.C. [grant number H30].

Disclosures

The authors have no conflict of interest to declare.

Acknowledgements

We are grateful to Division of Gene Research, Research Center for Advanced Science and Technology in Shinshu University, for supporting the present study.

References

Batistic, O., Waadt, R., Steinhorst, L., Held, K. and Kudla, J. (2010) CBL-mediated targeting of CIPKs facilitates the decoding of calcium signals emanating from distinct cellular stores. *Plant J* 61: 211-222.

Berthomieu, P., Conejero, G., Nublat, A., Brackenbury, W.J., Lambert, C., Savio, C., et al. (2003) Functional analysis of AtHKT1 in *Arabidopsis* shows that Na^+ recirculation by the phloem is crucial for salt tolerance. *EMBO J.* 22: 2004-2014.

Bowman, J.L. (2016a) A brief history of *Marchantia* from greece to genomics. *Plant Cell Physiol* 57: 210-229.

Bowman, J.L., Araki, T., Arteaga-Vazquez, M.A., Berger, F., Dolan, L., Haseloff, J., et al. (2016b) The naming of names: guidelines for gene nomenclature in *Marchantia*. *Plant Cell Physiol* 57: 257-261.

Bowman, J.L., Kohchi, T., Yamato, K.T., Jenkins, J., Shu, S., Ishizaki, K., et al. (2017) Insights into land plant evolution garnered from the *Marchantia polymorpha* genome. *Cell* 171: 287-304 e215.

Campbell, M.T., Bandillo, N., Al Shiblawi, F.R.A., Sharma, S., Liu, K., Du, Q., et al. (2017) Allelic variants of OsHKT1;1 underlie the divergence between indica and japonica subspecies of rice (*Oryza sativa*) for root sodium content. *PLoS genetics* 13: e1006823.

Cao, Y., Liang, X., Yin, P., Zhang, M. and Jiang, C. (2019) A domestication-associated reduction in K^+-preferring HKT transporter activity underlies maize shoot K^+ accumulation and salt tolerance. *New Phytol* 222: 301-317.

Corratgé-Faillie, C., Jabnoune, M., Zimmermann, S., Very, A.A., Fizames, C. and Sentenac, H. (2010) Potassium and sodium transport in non-animal cells: the Trk/Ktr/HKT transporter family. *Cell Mol Life Sci* 67: 2511-2532.

Corratgé, C., Zimmermann, S., Lambilliotte, R.R.L., Plassard, C., Marmeisse, R., Thibaud, J.B., et al. (2007) Molecular and functional characterization of a Na^+-K_+ transporter from the Trk family in the ectomycorrhizal fungus *Hebeloma cylindrosporumk. J. Biol. Chem.* 282: 26057-26066.

Davenport, R.J., Munoz-Mayor, A., Jha, D., Essah, P.A., Rus, A. and Tester, M. (2007) The Na^+ transporter AtHKT1;1 controls retrieval of Na^+ from the xylem in *Arabidopsis*. *Plant Cell Environ* 30: 497-507.

Durell, S.R. and Guy, H.R. (1999) Structural models of the KtrB, TrkH, and Trk1,2 symporters based on the structure of the KcsA K^+ channel. *Biophys J* 77: 789-807.

Durell, S.R., Hao, Y., Nakamura, T., Bakker, E.P. and Guy, H.R. (1999) Evolutionary relationship between K^+ channels and symporters. *Biophys J* 77: 775-788.

Gamborg, O.L., Miller, R.A. and Ojima, K. (1968) Nutrient requirements of suspension cultures of soybean root cells. *Exp Cell Res* 50: 151-158.

Gassmann, W., Rubio, F. and Schroeder, J.I. (1996) Alkali cation selectivity of the wheat root high-affinity potassium transporter HKT1. *Plant J* 10: 869-52.

Haro, R., Banuelos, M.A. and Rodriguez-Navarro, A. (2010) High-affinity sodium uptake in land plants. *Plant Cell Physiol* 51: 68-79.

Hauser, F. and Horie, T. (2010) A conserved primary salt tolerance mechanism mediated by HKT transporters: a mechanism for sodium exclusion and maintenance of high K/Na ratio in leaves during salinity stress. *Plant Cell Environ* 33: 552-565.

Held, K., Pascaud, F., Eckert, C., Gajdanowicz, P., Hashimoto, K., Corratge-Faillie, C., et al. (2011) Calcium-dependent modulation and plasma membrane targeting of the AKT2 potassium channel by the CBL4/CIPK6 calcium sensor/protein kinase complex. *Cell Res.* 21: 1116-1130.

Horie, T., Costa, A., Kim, T.H., Han, M.J., Horie, R., Leung, H.Y., et al. (2007) Rice OsHKT2;1 transporter mediates large Na^+ influx component into K^+-starved roots for growth. *EMBO J.* 26: 3003-3014.

Horie, T., Hauser, F. and Schroeder, J.I. (2009) HKT transporter-mediated salinity resistance mechanisms in *Arabidopsis* and monocot crop plants. *Trends in plant science* 14: 660-668.

Horie, T., Yoshida, K., Nakayama, H., Yamada, K., Oiki, S. and Shinmyo, A. (2001) Two types of HKT

transporters with different properties of Na^+ and K^+ transport in *Oryza sativa. Plant J.* 27: 129-138.
Ishizaki, K. (2017) Evolution of land plants: insights from molecular studies on basal lineages. *Biosci Biotechnol Biochem* 81: 73-80.
Ishizaki, K., Chiyoda, S., Yamato, K.T. and Kohchi, T. (2008) Agrobacterium-mediated transformation of the haploid liverwort *Marchantia polymorpha* L., an emerging model for plant biology. *Plant Cell Physiol* 49: 1084-1091.
Ishizaki, K., Nishihama, R., Ueda, M., Inoue, K., Ishida, S., Nishimura, Y., et al. (2015) Development of gateway binary vector series with four different selection markers for the liverwort *Marchantia polymorpha*. *PLoS One* 10: e0138876.
Ishizaki, K., Nishihama, R., Yamato, K.T. and Kohchi, T. (2016) Molecular genetic tools and techniques for *Marchantia polymorpha* research. *Plant Cell Physiol* 57: 262-270.
Ismail, A.M. and Horie, T. (2017) Genomics, physiology, and molecular breeding approaches for improving salt tolerance. *Annual review of plant biology* 68: 405-434.
Karahara, I. and Horie, T. (2021) Functions and structure of roots and their contributions to salinity tolerance in plants. *Breed Sci* 71: 89-108.
Kawakami, Y., Imran, S., Katsuhara, M. and Tada, Y. (2020) Na^+ transporter SvHKT1;1 from a halophytic turf grass is specifically upregulated by high Na^+ concentration and regulates shoot Na^+ concentration. *Int J Mol Sci* 21.
Kobayashi, N.I., Yamaji, N., Yamamoto, H., Okubo, K., Ueno, H., Costa, A., et al. (2017) OsHKT1;5 mediates Na^+ exclusion in the vasculature to protect leaf blades and reproductive tissues from salt toxicity in rice. *Plant J.* 91: 657-670.
Kohchi, T., Yamato, K.T., Ishizaki, K., Yamaoka, S. and Nishihama, R. (2021) Development and Molecular Genetics of *Marchantia polymorpha*. *Annu Rev Plant Biol* 72: 677-702.
Kubota, A., Ishizaki, K., Hosaka, M. and Kohchi, T. (2013) Efficient Agrobacterium-mediated transformation of the liverwort *Marchantia polymorpha* using regenerating thalli. *Biosci Biotechnol Biochem* 77: 167-172.
Kumar, S., Stecher, G. and Tamura, K. (2016) MEGA7: Molecular evolutionary genetics analysis version 7.0 for bigger datasets. *Mol Biol Evol* 33: 1870-1874.
Laurie, S., Feeney, K.A., Maathuis, F.J., Heard, P.J., Brown, S.J. and Leigh, R.A. (2002) A role for HKT1 in sodium uptake by wheat roots. *Plant J.* 32: 139-149.
Mäser, P., Eckelman, B., Vaidyanathan, R., Horie, T., Fairbairn, D.J., Kubo, M., et al. (2002a) Altered shoot/root Na^+ distribution and bifurcating salt sensitivity in *Arabidopsis* by genetic disruption of the Na^+ transporter AtHKT1. *FEBS Lett* 531: 157-161.
Mäser, P., Hosoo, Y., Goshima, S., Horie, T., Eckelman, B., Yamada, K., et al. (2002b) Glycine residues in potassium channel-like selectivity filters determine potassium selectivity in four-loop-per-subunit HKT transporters from plants. *Proc. Natl. Acad. Sci. U.S.A.* 99: 6428-6433.
Mian, A., Oomen, R.J., Isayenkov, S., Sentenac, H., Maathuis, F.J. and Very, A.A. (2011) Over-expression of an Na^+-and K^+-permeable HKT transporter in barley improves salt tolerance. *Plant J* 68: 468-479.
Omasits, U., Ahrens, C.H., Muller, S. and Wollscheid, B. (2014) Protter: interactive protein feature visualization and integration with experimental proteomic data. *Bioinformatics* 30: 884-886.
Platten, J.D., Cotsaftis, O., Berthomieu, P., Bohnert, H., Davenport, R.J., Fairbairn, D.J., et al. (2006) Nomenclature for HKT transporters, key determinants of plant salinity tolerance. *Trends in plant science* 11: 372-374.
Preston, G.M., Carroll, T.P., Guggino, W.B. and Agre, P. (1992) Appearance of water channels in *Xenopus* oocytes expressing red cell CHIP28 protein. *Science* 256: 385-387.
Ren, Z.H., Gao, J.P., Li, L.G., Cai, X.L., Huang, W., Chao, D.Y., et al. (2005) A rice quantitative trait locus for salt tolerance encodes a sodium transporter. *Nat. Genet.* 37: 1141-1146.
Riedelsberger, J., Miller, J.K., Valdebenito-Maturana, B., Pineros, M.A., Gonzalez, W. and Dreyer, I. (2021) Plant HKT channels: an updated view on structure, function and gene regulation. *Int J Mol Sci* 22.
Saint-Marcoux, D., Proust, H., Dolan, L. and Langdale, J.A. (2015) Identification of reference genes for real-time quantitative PCR experiments in the liverwort *PLoS One* 10: e0118678.
Shimamura, M. (2016) *Marchantia polymorpha*: taxonomy, phylogeny and morphology of a model system. *Plant Cell Physiol* 57: 230-256.
Su, Y., Luo, W., Lin, W., Ma, L. and Kabir, M.H. (2015) Model of cation transportation mediated by high-affinity potassium transporters (HKTs) in higher plants. *Biol. Proced* 17: 1.
Sunarpi, Horie, T., Motoda, J., Kubo, M., Yang, H., Yoda, K., et al. (2005) Enhanced salt tolerance mediated by AtHKT1 transporter-induced Na^+ unloading from xylem vessels to xylem parenchyma cells. *Plant J.* 44: 928-938.

Suzuki, K., Yamaji, N., Costa, A., Okuma, E., Kobayashi, N.I., Kashiwagi, T., et al. (2016) OsHKT1;4-mediated Na^+ transport in stems contributes to Na^+ exclusion from leaf blades of rice at the reproductive growth stage upon salt stress. *BMC Plant Biol.* 16: 22.

Tsuboyama-Tanaka, S. and Kodama, Y. (2015) AgarTrap-mediated genetic transformation using intact gemmae/gemmalings of the liverwort *Marchantia polymorpha* L. *J Plant Res* 128: 337-344.

Uozumi, N., Kim, E.J., Rubio, F., Yamaguchi, T., Muto, S., Tsuboi, A., Bakker, E.P., Nakamura, T. and Schroeder, J.I. (2000) The Arabidopsis *HKT1* gene homolog mediates inward Na^+ currents in *Xenopus laevis* oocytes and Na^+ uptake in *Saccharomyces cerevisiae*. *Plant Physiol* 122: 1249-1259.

Wang, R., Jing, W., Xiao, L., Jin, Y., Shen, L. and Zhang, W. (2015) The rice high-affinity potassium transporter1;1 is involved in salt tolerance and regulated by an MYB-type transcription factor. *Plant physiology* 168: 1076-1090.

Xue, S., Yao, X., Luo, W., Jha, D., Tester, M., Horie, T., et al. (2011) AtHKT1;1 mediates nernstian sodium channel transport properties in Arabidopsis root stelar cells. *PLoS One* 6: e24725.

Yao, X., Horie, T., Xue, S., Leung, H.Y., Katsuhara, M., Brodsky, D.E., et al. (2010) Differential sodium and potassium transport selectivities of the rice OsHKT2;1 and OsHKT2;2 transporters in plant cells. *Plant Physiol* 152: 341-355.

Zhang, M., Cao, Y., Wang, Z., Wang, Z.Q., Shi, J., Liang, X., et al. (2018) A retrotransposon in an HKT1 family sodium transporter causes variation of leaf Na^+ exclusion and salt tolerance in maize. *New Phytol* 217: 1161-1176.

Zhang, Y., Su, J., Duan, S., Ao, Y., Dai, J., Liu, J., et al. (2011) A highly efficient rice green tissue protoplast system for transient gene expression and studying light/chloroplast-related processes. *Plant methods.* 7: 30.

Figure Captions

Fig. 1 Phylogenetic relationships of plant HKT transporters. Maximum likelihood phylogenetic tree of 31 HKT proteins from herbaceous plants and bryophytes. The tree was constructed using MEGA 7 (Kumar et al. 2016) with 1,000 bootstrap trials. The scale bar represents 0.2 substitutions per site. Abbreviations of scientific names: At: *Arabidopsis thaliana*; Gm: *Glycine max*; Hv: *Hordeum vulgare*; Mp: *Marchantia polymorpha*; Mt: *Medicago truncatula;* Os: *Oryza sativa*; Pha: *Phragmites australis*; Sb: *Sorghum bicolor*; Sm: *Selaginella moellendorffii*; Ta: *Triticum aestivum*; Tm: *T. monococcum*; Pp: *Physcomitrium patens*.

Fig. 2 Structure of the MpHKT1 protein. (A) The predicted secondary structure of MpHKT1, comprising 812 amino acids. (B) The predicted secondary structure of truncated-MpHKT1 (t-MpHKT1), comprising 595 amino acids. Secondary structures of MpHKT1 proteins were predicted using Protter (http://wlab.ethz.ch/protter/start/) (Omasits et al. 2014). The numbers in panels A and B indicate transmembrane domains; PM: plasma membrane. (C) Alignments of amino acids that constitute filter-pore-forming regions (p-loops: P_A to P_D) in HKT proteins. Arrowheads indicate the key amino acids, which are a major determinant of K^+ selectivity (Mäser et al. 2002b). See the caption of Fig. 1 for abbreviations of scientific names.

Fig. 3 Subcellular localization of enhanced green fluorescent protein (EGFP)-fused MpHKT1 transporters in a plant cell. EGFP-MpHKT1 or EGFP-t-MpHKT1 was transiently overexpressed in protoplasts prepared from leaf sheaths of rice seedlings as described previously (Kobayashi et al. 2017). EGFP or EGFP-MpHKT1 proteins were co-expressed with CBL1n-OFP (orange fluorescent protein), which is used as a PM marker. EGFP-derived fluorescence from a single focal plane of one representative rice protoplast expressing either EGFP-MpHKT1 (A), EGFP-t-MpHKT1 (B), or EGFP alone (C). OFP-derived fluorescence from EGFP-MpHKT1 (D), EGFP-t-MpHKT1 (E), or EGFP (F). Merged images of EGFP- and OFP-derived fluorescence: EGFP-MpHKT1 (G), EGFP-t-MpHKT1 (H), or EGFP (I). (J-L) Results of the plot-profile pixel intensity analysis of protoplasts expressing the different constructs (magenta and green colors represent fluorescence

from OFP and EGFP, respectively): EGFP-MpHKT1 (J), EGFP-t-MpHKT1 (K), or EGFP (L). Brightfield images of the protoplast expressing EGFP-MpHKT1 (M), EGFP-t-MpHKT1 (N), or EGFP alone (O).

Fig. 4 Monovalent alkaline cation selectivity of MpHKT1 proteins. The two-electrode voltage clamp experiment using *Xenopus laevis* oocytes were conducted. Current–voltage relationships (I-V curves) obtained from oocytes injected with either water (A), 12.5 ng Mp*HKT1* cRNA (B), or 12.5 ng *t*-Mp*HKT1* cRNA (C) are shown. External bath solutions contained Na^+, K^+, Cs^+, Rb^+, or Li^+ (as 96 mM chloride salts). Basic background elements in the bath solution are 1.8 mM $CaCl_2$, 1.8 mM $MgCl_2$, 1.8 mM mannitol, and 10 mM HEPES (pH 7.5 with Tris). Voltage steps ranged from −150 to +30 mV with 15-mV increments. Data are shown as means ± SE (n = 5 for A and n = 13-14 for B and C). Each inset indicates I-V curves ranging from 0 mV to -60 mV to highlight the reversal potentials in each bath solution.

Fig. 5 Effects of monovalent alkaline cations on MpHKT1-mediated Na^+ transport. I-V curves obtained from oocytes injected with either 12.5 ng Mp*HKT1* cRNA (A), 12.5 ng *t*-Mp*HKT1* cRNA (B), or water (inset in B). (C) Box plot of ionic conductance calculated from a part of the data presented in A (V = from -90 to -150 mV). (D) Box plot of the ionic conductance calculated from a part of the data presented in B (the same range as C). The external solutions used for the recordings contained 96 mM NaCl, 72 mM NaCl + 24 mM KCl, 72mM NaCl + 24 mM RbCl, 72 mM NaCl + 24 mM CsCl, 72 mM NaCl + 24 mM LiCl, or 72 mM NaCl. Basic background elements in the bath solution are 1.8 mM $CaCl_2$, 1.8 mM $MgCl_2$, 1.8 mM mannitol, and 10 mM HEPES (pH 7.5 with Tris). Voltage steps ranged from −150 to +30 mV with 15-mV increments. Data are the means ± SE (n = 10 for A and B, and n = 5 for water). Different letters indicate significant differences ($p < 0.05$).

Fig. 6 Quantitative real time PCR (qPCR) analysis on Mp*HKT1* expression. (A) Relative expression levels of Mp*HKT1* in male (Tak-1) and female (Tak-2) accessions of *M. polymorpha* grown under high (15 mM) and low (0.05 mM) K^+ conditions with or without 50 mM NaCl. (B) Relative expression levels of Mp*HKT1* in Tak-1 and

transgenic *M. polymorpha* lines overexpressing Mp*HKT1* grown on half-strength Gamborg's B5 medium (15 mM K^+). Note that OE and t-OE, respectively, represent overexpression of MpHKT1 and t-MpHKT1. The Mp*EF1α* transcript was analyzed as an internal control (Saint-Marcoux et al. 2015) in parallel with Mp*HKT1*. Two independent individuals per line were used and qPCR was repeated three times using each individual in all experiments (n = 6, in total). Error bars represent standard deviation and different letters represent significant differences at $p < 0.05$ (Tukey's test).

Fig. 7 Na^+ and K^+ contents in male WT and transgenic WT overexpressing MpHKT1 transporters under various K^+ and Na^+ conditions (n = 6–12 ± SD). (A) The Na^+ content of each line under a 15 mM K^+ condition. (B) The Na^+ content of each line under a 15 mM K^+ + 50 mM Na^+ condition. (C) The K^+ content of each line under a 15 mM K^+ condition. (D) The K^+ content of each line under a 15 mM K^+ + 50 mM Na^+ condition. (E) The Na^+ content of each line under a 0.5 mM K^+ condition. (F) The Na^+ content of each line under a 0.5 mM K^+ + 50 mM Na^+ condition. (G) The K^+ content of each line under a 0.5 mM K^+ condition. (H) The K^+ content of each line under a 0.5 mM K^+ + 50 mM Na^+ condition. OE and t-OE, respectively, represent overexpression of MpHKT1 and t-MpHKT1. Error bars represent standard deviation and different letters represent significant differences at $p < 0.05$ (Tukey-Kramer's test).

Fig. 8 Increased salt sensitivity of *M. polymorpha* overexpressing MpHKT1. Elite young thalli of each line were grown on half-strength Gamborg's B5 medium using a nylon mesh for 10 days. Then, each nylon mesh was transferred on modified Gamborg's B5 medium that contains either 0.5 mM K^+ or 0.5 mM K^+ and 50 mM Na^+. Photographs were taken after three weeks. Six independent individuals were tested, and a representative result was shown: (A) 0.5 K^+; (B) 0.5 mM K^+ and 50 mM Na^+. Fresh weights were measured immediately after this: (C) 0.5 K^+; (D) 0.5 mM K^+ and 50 mM Na^+ (n = 6 ± SD). Different letters represent significant differences at $p < 0.05$ (Tukey's test).

Fig. 9 $^{22}Na^{+}$ tracer experiments using male WT and transgenic WT overexpressing MpHKT1 transporters. All lines were placed on the medium containing 0.5 mM K^{+}, 50 mM Na^{+}, and $^{22}Na^{+}$ (1.85 kBq/ml) for 1 h. The Na^{+} uptake rate (nmol mg^{-1} h^{-1}) was calculated. (A) Images of the six individuals used for this $^{22}Na^{+}$ tracer study: a photograph taken after the $^{22}NaCl$ absorption (left) and a spatial distribution of $^{22}Na^{+}$ visualized using an imaging plate (right). (B) Box plot summary of the Na^{+} uptake rate (nmol mg^{-1} h^{-1}; n = 6). OE and t-OE, respectively, represent overexpression of MpHKT1 and t-MpHKT1. Different letters represent significant differences at $p < 0.05$ (Tukey's test).

Figure 1

Figure 2

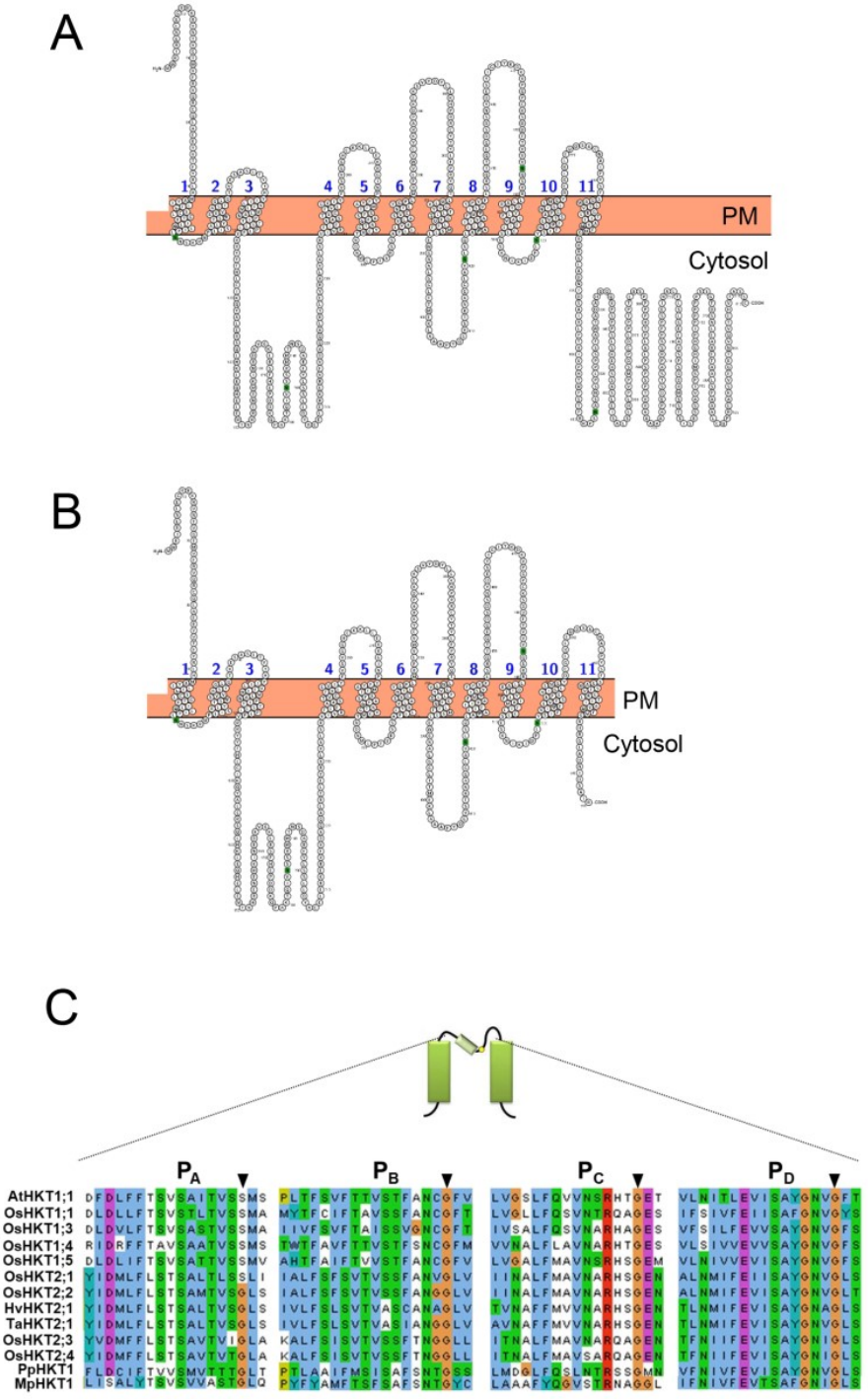

Figure 3

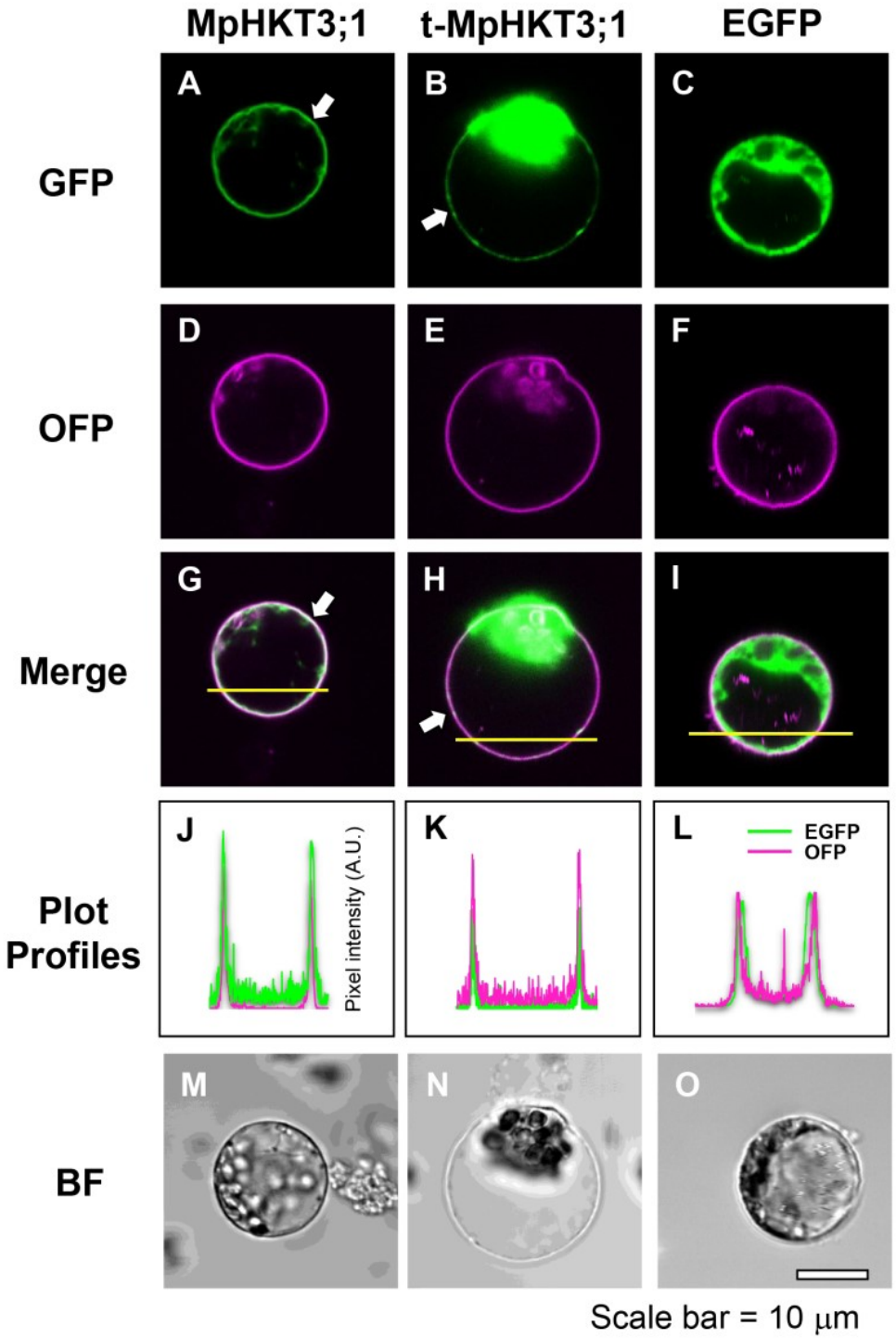

Figure 4

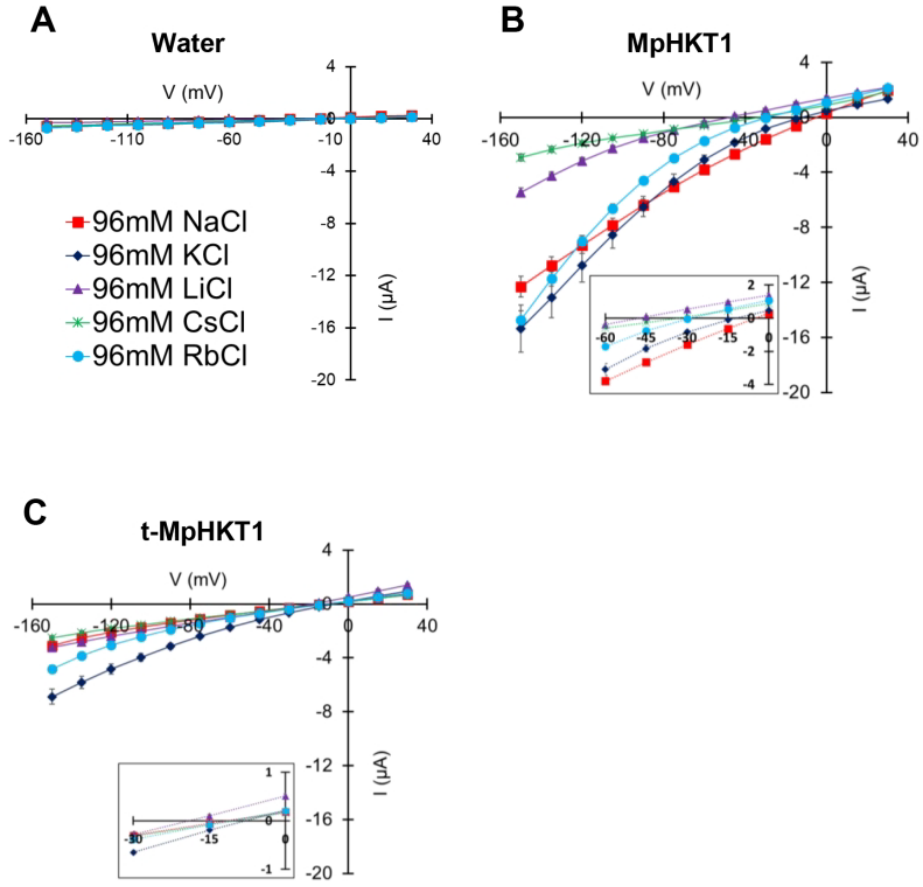

Figure 5

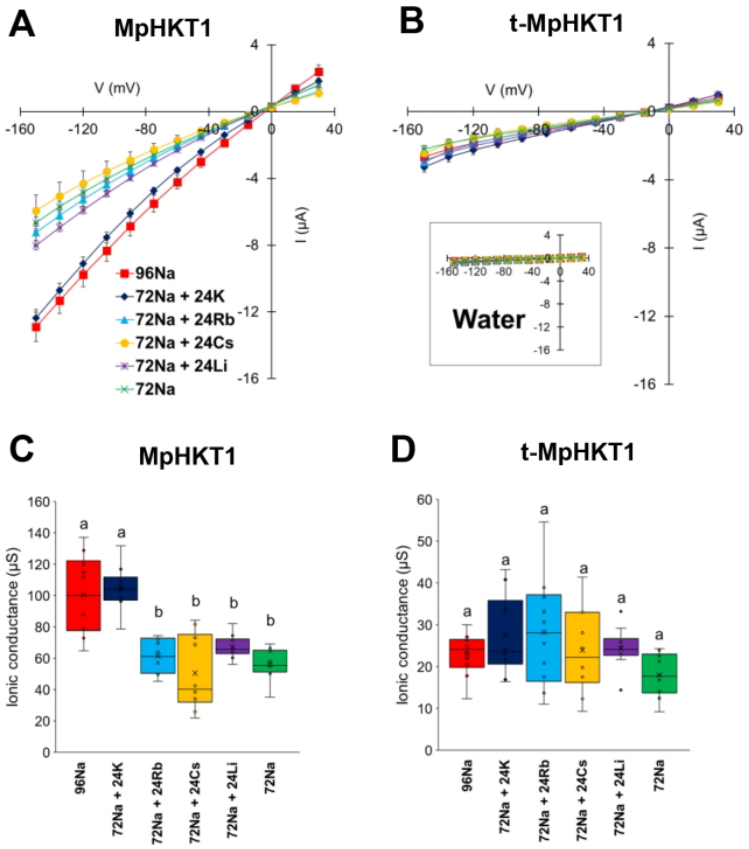

Figure 6

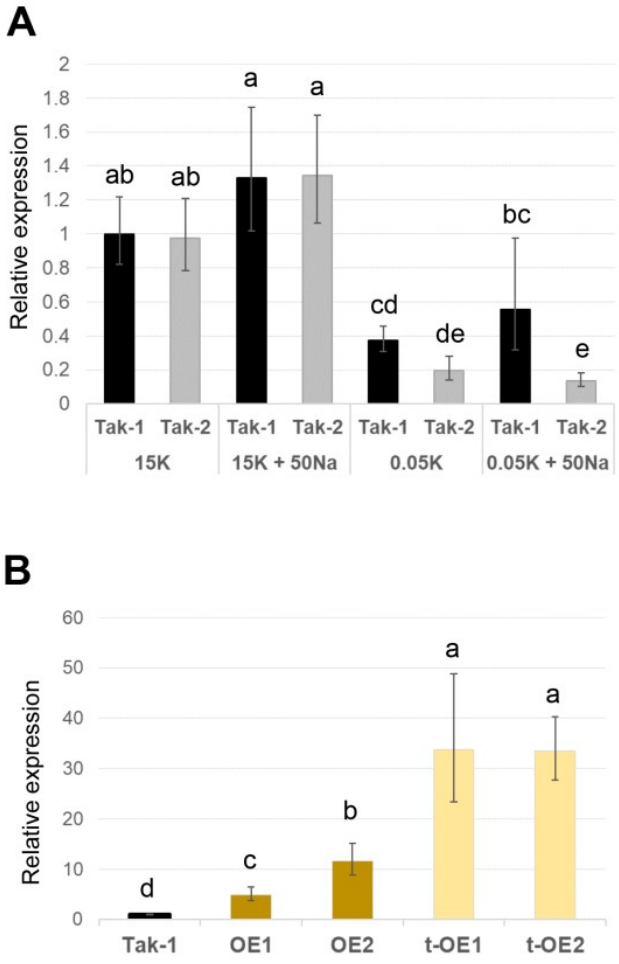

Figure 7

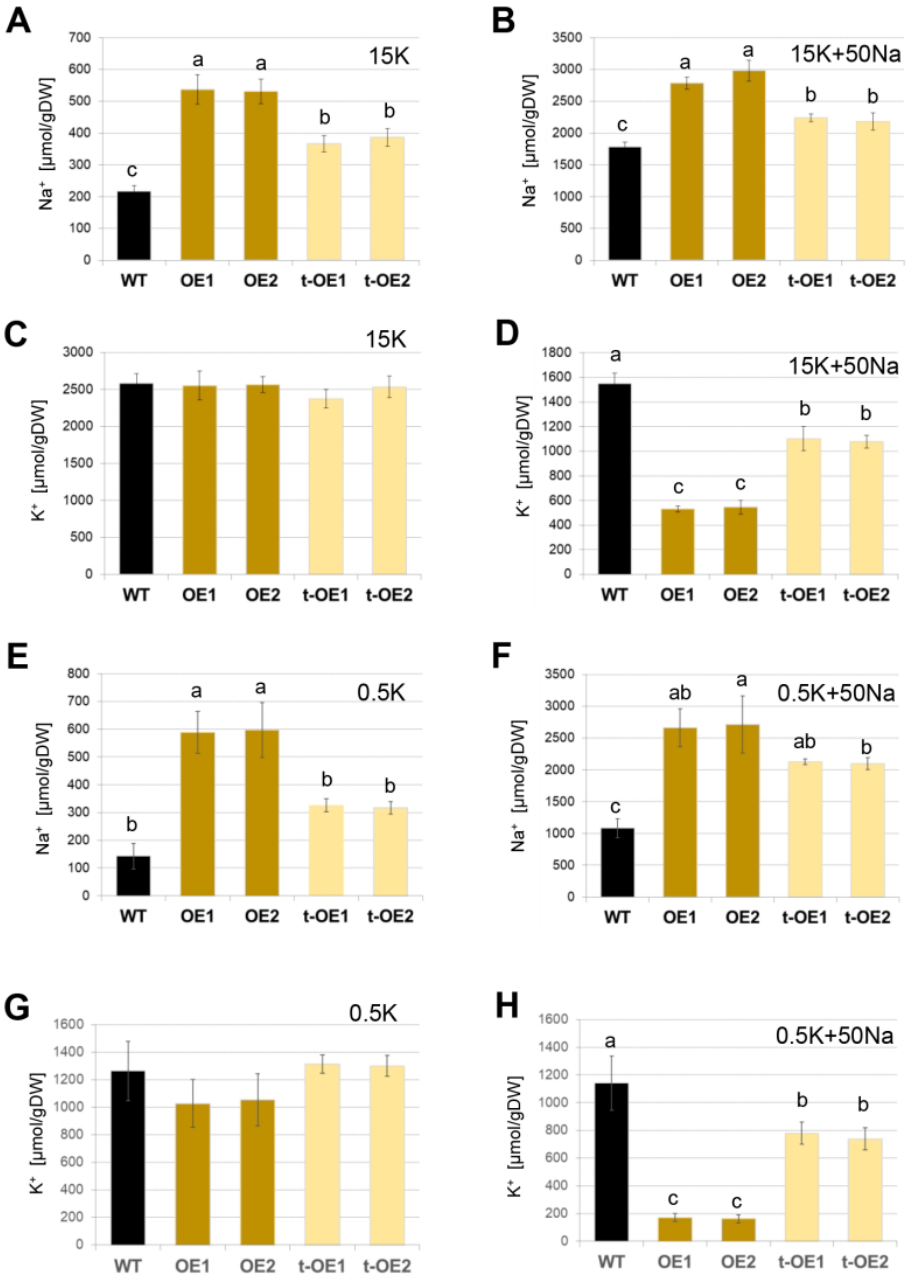

Figure 8

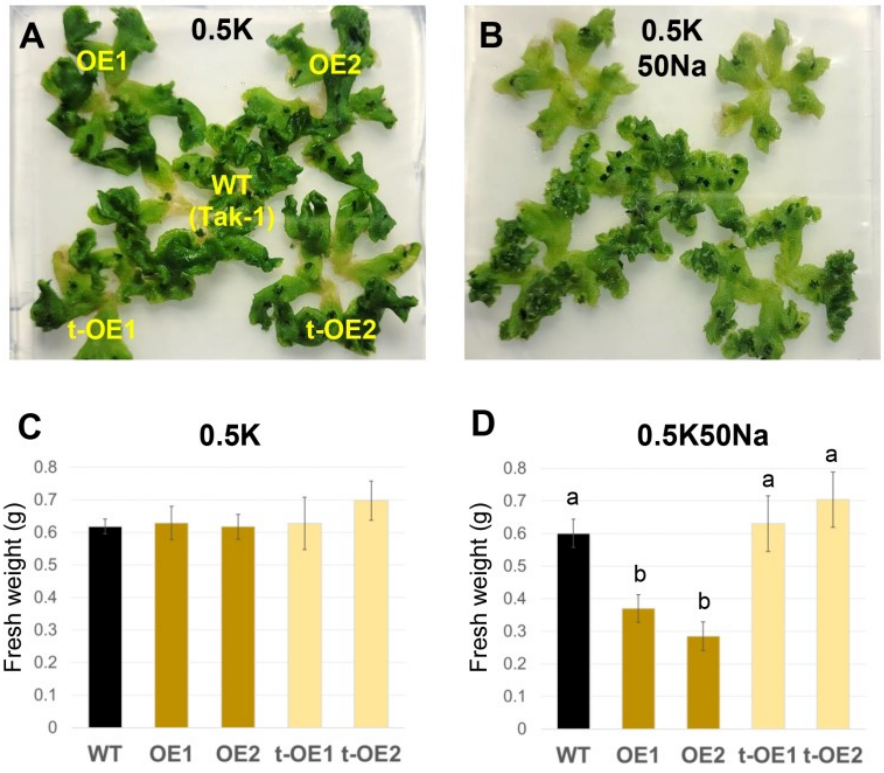

Figure 9